



EUROfusion

WPHCD-CPR(18) 20353

R Jacquier et al.

**An innovative helicon plasma source for
an alternative concept of DEMO
negative ion beam injector**

Preprint of Paper to be submitted for publication in Proceeding of
30th Symposium on Fusion Technology (SOFT)



This work has been carried out within the framework of the EUROfusion Consortium and has received funding from the Euratom research and training programme 2014-2018 under grant agreement No 633053. The views and opinions expressed herein do not necessarily reflect those of the European Commission.

This document is intended for publication in the open literature. It is made available on the clear understanding that it may not be further circulated and extracts or references may not be published prior to publication of the original when applicable, or without the consent of the Publications Officer, EUROfusion Programme Management Unit, Culham Science Centre, Abingdon, Oxon, OX14 3DB, UK or e-mail Publications.Officer@euro-fusion.org

Enquiries about Copyright and reproduction should be addressed to the Publications Officer, EUROfusion Programme Management Unit, Culham Science Centre, Abingdon, Oxon, OX14 3DB, UK or e-mail Publications.Officer@euro-fusion.org

The contents of this preprint and all other EUROfusion Preprints, Reports and Conference Papers are available to view online free at <http://www.euro-fusionscipub.org>. This site has full search facilities and e-mail alert options. In the JET specific papers the diagrams contained within the PDFs on this site are hyperlinked

An innovative helicon plasma source for an alternative concept of DEMO Negative Ion Beam

Rémy Jacquier^a, Riccardo Agnello^a, Basile Duteil^a, Claudio Marini^a, Philippe Guittienne^b, Alan Howling^a, Ivo Furno^a, Gennady Plyushchev^a, Alain Simonin^c, Iaroslav Morgal^c, Stephane Bechu^d

^aEcole Polytechnique Fédérale de Lausanne (EPFL), Swiss Plasma Center (SPC), CH-1015 Lausanne, Switzerland

^bHelyssen, Belmont-sur-Lausanne, Switzerland

^cIRFM, CEA, Saint-Paul-lez-Durance, France

^dLSPC, CNRS/IN2P3, Grenoble, France

Neutral Beam Injectors (NBI) for DEMO-like reactors will need deuterium neutrals at a high energy (>0.8 MeV) and a fair injector overall efficiency (>50 %) for plasma heating and current drive. In order to achieve this, negative ion injectors will be required. A conceptual design of injectors (SIPHORE at IRFM, CEA, in France) expects to extract negative deuterium ions and photo-neutralize the accelerated D-

In this context, the Swiss Plasma Center of EPFL is developing an innovative helicon device (RAID: Resonant Antenna Ion Device), which provides a quasi-homogeneous electron density along the axial direction and is able to produce negative ions in the plasma volume (10^{16} m⁻³).

In RAID reactor, the helicon wave is sustained by a resonant antenna plasma source at 13.56 MHz (input power ≤ 10 kW), connected to a cylindrical vacuum chamber (1.5 m long, 0.4 m diameter) surrounded by 6 Helmholtz coils, providing a DC magnetic field up to 800 G on axis. This paper deals with the propagation of helicon wave measurements using a three-axis magnetic probe. In typical H₂ plasmas (0.3 Pa), the helicon wave is right-handed polarized with a wavelength of 240 mm.

Keywords: plasma, source, resonant antenna, helicon, magnetic probe, wave.

1. Introduction

Neutral Beam Injectors (NBI) for DEMO-like reactors will need deuterium neutrals at a high energy (>0.8 MeV) and a fair injector overall efficiency (>50 %) for plasma heating and current drive [1-3]. The neutralization efficiency of positive ions drops for energies higher than 100 keV/nucleon and thus NBIs based on negative ions are required [4]. A conceptual design of injectors (SIPHORE at IRFM, CEA, Cadarache, France) expects to extract negative deuterium ions from a plasma 3 m long and 15 cm wide, and to photo-neutralize the accelerated D⁻ [2,3]. The Swiss Plasma Center (SPC) of EPFL has developed a helicon device (RAID: Resonant Antenna Ion Device) as a test bench of plasma sources for this new concept of NBI injectors [5].

On RAID, a birdcage resonant antenna is used to generate and sustain the plasma [6]. The electromagnetic configuration created by the resonant source and the axial DC magnetic field enables the propagation of a bounded type of whistler wave, called a helicon wave [7]. There are several reasons to use a helicon source instead of conventional inductive coils. Firstly, for the same power, an antenna in helicon mode provides an electron density around one order of magnitude higher than in inductive mode (typically 10^{18} m⁻³ in hydrogen and deuterium discharges [8,9]) although why this occurs is not fully understood yet. Secondly, the plasma can be maintained even at low pressure (<0.3 Pa), resulting in less wave damping and a quasi-homogeneous electron density along the plasma column. Moreover, in hydrogen and deuterium plasmas, a high degree of dissociation as well as a high volume production of negative ions was demonstrated.

These results are very promising for negative ion beam application for fusion.

Here, we present first helicon wave measurements on RAID in hydrogen plasmas. To measure the component of the RF magnetic field associated to the helicon wave, we have designed and built a high frequency magnetic probe (B-dot probe). Currently, the main challenge is achieving a high signal-to-noise ratio, with the smallest perturbation by the use of a miniaturized probe head. An accurate measurement of the induced current is performed by using a hybrid transformer, which reduces the capacitive parasitic pickup.

The next following chapters expand on the RAID device and its different diagnostics, the design and calibration of the B-dot probe and finally, preliminary results are given for our standard plasma parameters to demonstrate how a helicon wave is efficiently created in RAID.

2. Resonant Antenna Ion Device (RAID)

2.1 Design and configuration

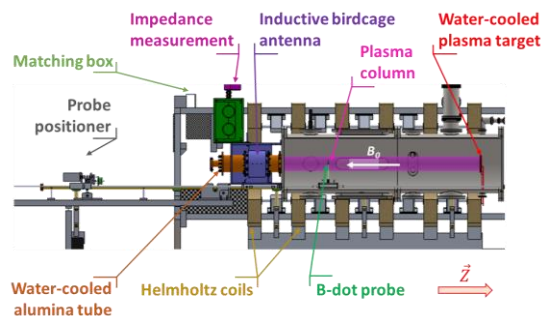


Fig. 1. RAID experiment with the main elements.

RAID, shown in Figure 1, is a linear device composed of a cylindrical vacuum chamber (1.5 m long and 0.4 m in diameter). It is pumped by a turbo-molecular and a backing pump below 10^{-6} mbar with a constant pumping speed of 170 l/s. Different gases (H_2 , D_2 , Ar and He) can be injected and the pressure during experiments is maintained at 0.3 Pa using a mass flow controller (the pressure usually required for NBI reactors).

The resonant source, a birdcage antenna located on the left side of the vacuum vessel, creates a plasma inside an alumina tube (40 cm long and 9.5 cm in diameter). An automatic T-matching circuit adapts the antenna impedance to the 50 ohm output impedance of the 13.56 MHz generator (15 kW maximum power).

The chamber is surrounded by five magnetic Helmholtz coils providing a DC magnetic field up to 800 G on axis. A sixth coil, around the antenna, produces a reversed field to generate a magnetic field gradient that helps plasma stabilization. When the helicon mode reaches 500 W, a plasma column is generated and sustained between the antenna and a copper target (see Figure 1), which absorbs most of the plasma energy. The vacuum vessel, the antenna, the matching box, the ceramic tube and the copper target are water-cooled.

2.2 The birdcage source

Birdcage antennas have been extensively studied for nuclear magnetic resonance [10]. The use of birdcage antennas as inductive plasmas source was first proposed by Ph. Guittienne [6] and first prototypes were developed in collaboration with the SPC [11]. It is a network of capacitors and copper tubes acting as RLC parallel resonant circuits. The antenna resonates at 13.56 MHz, generating a sinusoidal distribution of high current in the legs. This results in a uniform transverse RF magnetic field in the antenna interior, which efficiently excites helicon wave, a category of bounded whistler waves propagating in magnetized plasmas in the presence of an external axial DC magnetic field (see Figure 5).

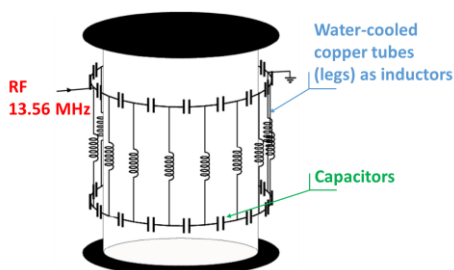


Fig. 2. Equivalent Radio Frequency (RF) circuit of the RAID antenna.

In pure inductive plasma mode, this system has been widely studied for industrial and research applications [11-14]. The high, purely-real input impedance around 140 ohm in vacuum drops with the plasma ignition to around 20 ohm and a small shift of the resonance frequency causes an imaginary component. This is due to the coupling of the network with the current induced in the plasma. The real input impedance facilitates the matching with the generator 50 Ohm output impedance with respect to a purely reactive load by diminishing the

current in the transmission line and thus decreasing the heating of the coaxial cable internal conductor. Moreover, it is scalable and the geometry of the network can be either cylindrical or planar [14].

2.3 Characterization of plasma profiles

In RAID, a number of diagnostics have been installed and successfully tested such as: Optical Emission Spectroscopy (OES), interferometry, cavity ring down spectroscopy, laser photo-detachment, laser induced fluorescence [15], Langmuir and magnetic probes. A probe positioner can move Langmuir or magnetic probes in axial and angular direction to obtain a three-dimensional (3D) full coverage of RAID plasmas (see Figures 1 and 3).

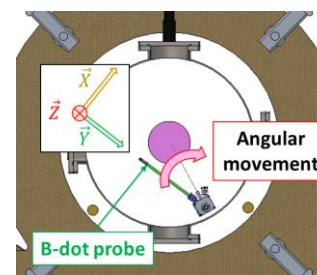


Fig. 3. Angular movement of the B-dot probe.

Profiles of electron temperature and density are shown in Figure 4 in a H_2 plasma, at 3 kW of power and a DC magnetic field of 200 G. Both profiles are quite homogeneous in the axial direction, as shown in Figure 4. The electron density on-axis, measured by interferometry, is in the order of $10^{18} m^{-3}$.

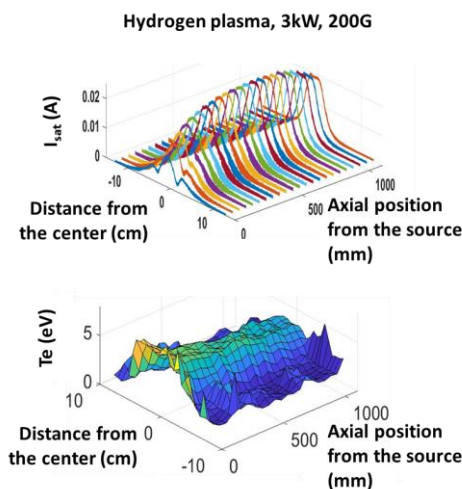


Fig. 4. 3D Ion saturation current and temperature profiles in RAID. The antenna is located at the axial position $z = 0$.

In the future SIPHORE experiment, this shape would be favorable for the extraction of a negative beam showing a sheet shape (3 m high, 1 cm wide) well adapted to the photo-neutralization concept [2,3]. Furthermore, the electron temperature in the center is high enough to excite raw vibrational states of H_2 molecules. These molecules diffuse towards the chamber wall in the lower temperature region, where dissociative attachment produces negative atomic ions. Thus, in H_2 plasmas, pressure 0.3 Pa and 3.5 kW RF power, a negative ion density of $2.3 \times 10^{16} m^{-3}$ and $3.3 \times 10^{16} m^{-3}$ have been respectively measured by OES [8] and cavity ring down spectroscopy [9]. At the same pressure, this is equivalent to the density obtained for 40 kW power in conventional

inductive source. Values of negative ion densities obtained at the same pressure with conventional inductive sources in volume production mode and with cesium seeding, although at much larger radio-frequency power, can be found in [16]. Today, it is not known how the extraction of negative ions from helicon device will react, but studies are ongoing in the IRFM at Cadarache. Furthermore, the deposition of wave energy is not fully understood and therefore requires analyzing wave properties. This stresses magnetic field measurements with B-dot probes, which will be described in the next section.

3. B-dot probe

3.1 Design of the B-dot

The B-dot is a magnetic probe dedicated to the measurement of the 3 components of the RF magnetic field in the plasma. It consists of 3 inductive pick-up coils, wrapped around a cubic probe head ($5 \times 5 \times 5 \text{ mm}^3$), made of ceramic. The Z coil measures the varying magnetic field in the axial direction of the RAID reactor while X and Y measure the fields in the cross section (see in Figure 3). The interpretation of the measurements is made from/by using Faraday's law:

$$V = -\frac{d\Phi_B}{dt}, \quad (1)$$

with Φ_B the magnetic flux linking a surface Σ , defined as:

$$\Phi_B = \int_{\Sigma} \mathbf{B}(\mathbf{r}, t) \cdot d\mathbf{A}, \quad (2)$$

where \mathbf{B} is the varying magnetic field and $d\mathbf{A}$ is an element of the surface area. Since the coil's cross-section is small enough:

$$V = -nA \frac{dB}{dt}, \quad (3)$$

where n is the number of turns and B is the component of the magnetic field perpendicular to the area A . Considering a harmonic time varying field $B(t) = |\widetilde{B}|e^{i\omega t}$, the amplitude of the probe voltage is:

$$V = -n\omega A |\widetilde{B}|. \quad (4)$$

At a specific frequency, nA is the calibration factor in the next section of this paper [17].

The B-dot should be designed as a non-perturbative probe, providing a reasonable signal-to-noise ratio with low parasitic signals. Probe coils, made of 3 turns, have a square section of $6 \times 6 \text{ mm}^2$. A twisted wire pair, an efficient method to cancel the parasitic inductive pick up

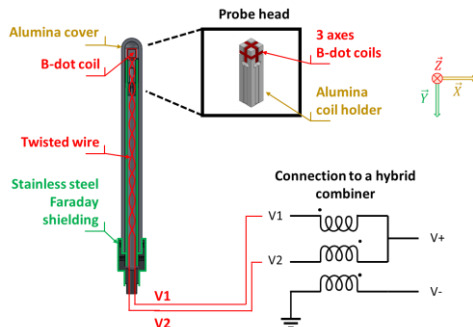


Fig. 4. B-dot connected to a hybrid combiner

in the line, connects each coil to a differential hybrid combiner (see Figure 4). To reduce the capacitive coupling of the wires to the plasma, a Faraday shield made of non-magnetic stainless steel screens the wires. The whole assembly is protected from plasma heating by an alumina cover.

The coil voltage signals also have common mode capacitive pick up, V_{cap} , due to a difference of potential between the plasma discharge and the coil. Therefore, the actual measurement of the coil voltage is $V = V_{ind} + V_{cap}$, with V_{ind} the magnetically induced voltage. To reduce the capacitive signal, we use a hybrid combiner [18]. V_1 and V_2 , voltages coming from both ends of one pick-up twisted pair, are inputs of the hybrid combiner made with trifilar windings on a toroidal ferrite core. One can easily verify that $V_1 - V_2 = V_+$ and $V_2 + V_1 = V_+$. As $V_- = V_+$, we have:

$$V_- = \frac{V_1 - V_2}{2} = V_{ind}, \quad (5)$$

$$V_+ = \frac{V_1 + V_2}{2} = V_{cap}. \quad (6)$$

3.2 Calibration on a test bench

To obtain an absolute value of the magnetic field and to compensate for small differences in geometry of the 3-axis pick up coils, it is necessary to calibrate this with a well-known magnetic field.

Calibration of the B-dot probe is performed using a birdcage antenna (Figure 5), which generates an oscillating magnetic field homogeneous in the cross section [10]. Figure 5 shows the amplitude of this magnetic field at one instant using a central cross section of the calibration birdcage.

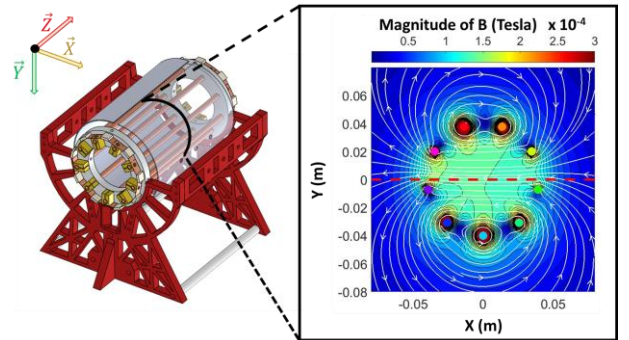


Fig. 5. Calibration antenna on the left and a model of the magnetic field magnitude in the central cross section on the right.

To compute the magnetic field lines with Faraday's law, the current distribution in the legs (copper tubes) is needed. To achieve this, the voltages at both ends of the legs are measured and the impedances of the legs are calculated taking into account the mutual inductances with the neighbours and of the cylindrical screens.

Each of the three B-dot coils is oriented in the direction of the uniform magnetic field of the calibration antenna. The B-dot voltages V are measured for different RF power injected into the calibration device to change the magnetic field intensity. Figure 6 is the resulting linear calibration of the B-dot with the calibration factors nA described in equation (4).

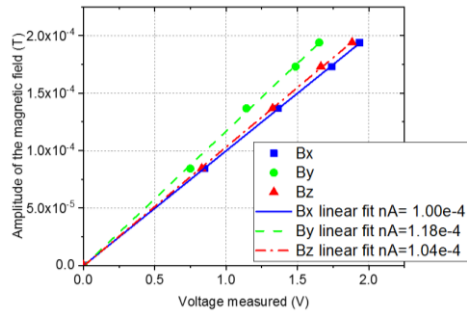


Fig. 6. Calibration curve of the B-dot probe.

3. First measurements in RAID

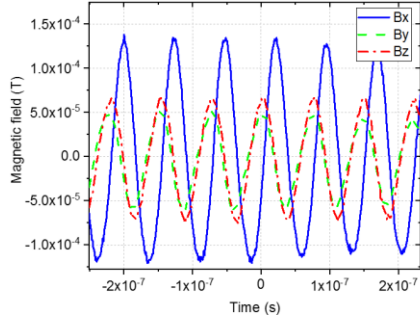


Fig. 7. Example of a time varying magnetic field.

Preliminary results obtained with the B-dot probe in RAID are discussed in this section. Figure 7 shows the time varying magnetic field at a fixed position (-10° from the centre angularly and 10 cm axially). This position corresponds to the edge of the plasma column. There are no measurements in the centre of the column because the wire used does not survive high temperatures (up to 700°C). The plasma is typical for the production of negative ions: H_2 plasma, 0.3 Pa, DC magnetic field 200 G and RF power 3 kW. As shown in the figure below, B_y leads B_x in phase.

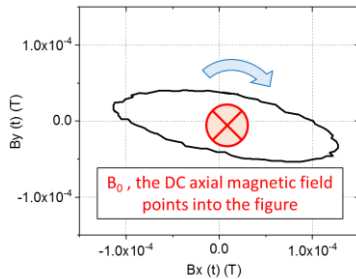


Fig. 8. Temporal polarization of the helicon wave

Thus, taking the direction of the DC magnetic field \vec{B}_0 as the reference, the temporal polarisation of the wave is right-handed (see Figure 8). This is in agreement with the standard measurements of helicon wave [7]. The last experiment done with the B-dot was an axial scan at a fixed RF phase and a fixed angular position (-10° from the centre) and the same plasma conditions as Figure 7. For this case, Figure 9 shows the amplitude of the magnetic field and highlights the wavelength of the wave, which can be measured at 240 mm.

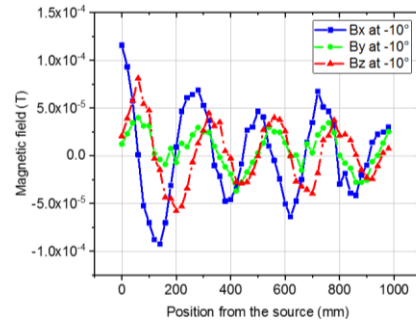


Fig. 9. Axial scan of the magnetic field.

These preliminary results demonstrate the potential of the B-dot probe for analysing the magnetic configuration of the helicon wave. In the near future, we will test other geometries of resonant antennas in order to choose the best source to match the requirements for NBIs injector sources. A full set of measurements as well as modelling will follow.

Acknowledgments

This work has been carried out within the framework of the EUROfusion Consortium and has received funding from the Euratom research and training programme 2014-2018 under grant agreement number 633053. The views and opinions expressed herein do not necessarily reflect those of the European Commission.

References

- [1] P. Sonato et al., *New J. Phys.* **18** (2016) 125002.
- [2] A. Simonin et al., *New J. Phys.* **18** (2016) 125005.
- [3] A. Simonin et al., *Nucl. Fusion* **55** (2015) 123020.
- [4] T. Inoue et al., *Nucl. Fusion* **46** (2006) 369.
- [5] I. Furno et al., Helicon wave-generated plasmas for negative ion beams for fusion, *EPJ Web of Conferences* **157** (2017) 03014.
- [6] Ph. Guittienne et al., *J. Appl. Phys.* **98** (2005) 083304.
- [7] R.W. Boswell, *Plasma Phys. Control. Fusion* **26** (1984) 1147.
- [8] C. Marini et al., *Nuc Fusion* **57** (2017) 036024.
- [9] R. Agnello et al., accepted for publication in *Rev. Sci. Instrum.*
- [10] J. Jin, *Electromagnetic analysis and designs in magnetic resonant imaging*, (Boca, Raton, FL: CRC Press), 1988.
- [11] Ch. Hollenstein et al., *Plasma Source Sci. Technol.* **22** (2013) 055021.
- [12] P. Demolon et al., *Vacuum*, **147** (2018) 58.
- [13] A. A. Howling et al., *Plasma Sources Sci. Technol.* **24** (2015) 065014.
- [14] Ph. Guittienne et al., *Plasma Sources Sci. Technol.* **24** (2015) 065015.
- [15] D. Thompson et al., *Phys. Plasmas* **24** (2017) 063517.
- [16] M. Berger et al., *Plasma Sources Sci. Technol.* **18** (2009) 025004.
- [17] M.P. Reilly et al., *Rev. Sci. Instrum.* **80** (2009) 053508.
- [18] G.G. Borg, *Rev. Sci. Instrum.* **65** (1994) 449.